Certain analysis for Grid current and Dc Capacitor voltage for Five -Terminal Hybrid AC/DC Microgrid Using ANFIS controller

[1]P.Shashavali [2]Ananya Bakkachinnayagari [3]N.Rajesh Kumar Gowd

[1 & 3]Assistant Professor, Dept. of EEE, S.K.U.College of Engg. & Tech., Ananthapuramu, Andhra Pradesh, India
[2] M.Tech Student, Dept. of EEE, S.K.U.College of Engg. & Tech., Ananthapuramu, Andhra Pradesh, India

***Abstract*:** In this paper deals with the performance of a three terminal and five terminal based Hybrid AC/DC micro grid by using ANFIS controller is proposed. By reducing the number of conversions CHB terminals are directly connected to the DAB converters. To improve Dc capacitor voltage and grid current two way of power conversion possible. The line frequency transformer included to the power transfer process to isolate DG's from the grid. The main problem was facing more conversion that impacts cost and number of stages and area size. To improve grid current and voltage zero sequence voltage controller, outer voltage controller, inner current controller, balancing voltage controller used. The power conversion can be operated vice-versa. The evaluation of results of three terminal and five terminal base CHB terminals by using MATLAB Simulink software.

Keywords: Three-terminal micro grid; five terminal microgrid; ANFIS controller; Hybrid AC/DC microgrid; DC Capacitor voltage; Outer Voltage Controller.

I. INTRODUCTION:

Due to the presence of DC power sources in microgrids such as PV, fuel cell, and energy storages, and modern DC loads, and considering the existing century-long AC power systems, interests on hybrid AC/DC microgrids are growing rapidly. These hybrid AC/DC microgrids contain AC/DC loads and power sources, have advantages of both AC and DC power systems, and are considered to be the most possible future distribution and transmission systems [5]- [7]. The hybrid grid consists of both AC and DC networks connected together by multi bidirectional converters. AC sources and loads are connected to the AC network where as DC sources and loads are tied to the DC network. The existing micro grids which are purely ac, the hybrid micro grid studied here comprises DC and AC sub grids interconnected by power electronic interfaces. The main challenge here is to manage power flows among all sources distributed throughout the two types of sub grids, which is certainly tougher than previous efforts developed for only AC or DC micro grid. This wider scope of control has not yet been investigated, and would certainly rely on the coordinated operation of dc sources, ac sources, and interlinking converters. The concept offers customers increased reliability and quality in the service provided by utility companies. However, the design of a micro grid architecture that provides an efficient operation poses a challenging problem. The conventional hybrid AC/DC microgrid include one AC transport and one DC transport [1], [2], [11], [13]. The AC and DC terminals are incorporated by means of three-section bidirectional AC/DC converter. The AC terminal include to the low-voltage application. Different AC/DC masses and DGs are identified with the relating AC/DC terminal. The line transformer is secured inside the power move way to disconnect DGs from the framework. Be that as it may, it has a few dangers, for example, enormous degree and weight, and staggering natural pollutants due to using transformer insulation oil, in comparison with excessive-frequency transformer. As the indispensable element, transformer insulation oil plays an important role in the insulation and cooling of power transformer [14]-[15]. To promote the direct integration of DGs and meet the increasing modern DC loads demand under the desired various DC bus voltages, multi-terminal hybrid AC/DC microgrid with one or more additional DC terminals is significantly necessary. Meanwhile, the recent trend of multi-terminal hybrid microgrid system is connected into three-phase medium-or high-voltage grid for larger power transfer capability and higher conversion efficiency.

To fulfill this requirement above, Cascaded H-bridge (CHB) converters can be used as the grid interface to directly transfer power to medium-voltage grid without line-frequency transformer [16]. In addition, dual active bridge (DAB) converters can be used as the DC microgrid interface for isolating the transmitted power and wide-range voltage conversion ratio. Thus, connection of CHB converters and DAB converters can be applied in the hybrid AC/DC microgrid. In order to lessen equipment estimation of intensity hardware gadgets with diminished assortment of energy transformation levels and meet the prerequisite of medium-voltage bundles without line-recurrence transformer combination, a 3-terminal half and half AC/DC microgrid structure is proposed to improve the proficiency and adaptability of vitality switch. In the three-terminal and 5-terminal half and half AC/DC microgrid related to medium-voltage grid, the proposed topology and novel control technique are demonstrated for simultaneous AC grid-cutting-edge what's more, DC capacitor voltage adjusting, even inside the serious case with very disoriented DC energy and network voltage droops.

In existing system three-terminal hybrid AC/DC microgrid with two DC ports (DC port1 and DC port2) and one AC port can be straight forwardly associated into three-stage medium voltage network. It comprises of the AC/DC converter (CHB converters) and the minimal DC/DC converter (DAB converters), made out of two cascaded of DC/DC converters, to be specific DC/DC converter-1 and DC/DC converter-2. Considering the impact of various connection patterns of DAB converters, namely different wire connection between CHB converters outputs and DAB converters inputs, and different DAB sub modules numbers in each DC/DC converter, the proposed three-terminal hybrid AC/DC microgrid has various types of internal structures. The DAB converter branches in various loads can be connected to the CHB cells' outputs randomly, where the issue of capacitor voltage unbalance will be solved by the proposed control scheme. Thus, the DAB converter connection patterns are not illustrated in Fig. 2. In order to clearly describe the power flow condition of DC microgrids, the DC microgrid-1 and DC microgrid-2 are replaced by

load-1 and load-2, respectively. Each phase of CHB converters consists of 4 cells, whose DC capacitor voltage are defined as *Vdcj* (*j*=1, 2… 12). The DC/DC converters are connected to the DC outputs of the front-end CHB structure. Each DC/DC converter consists of six parallel-related DAB converters. In DC/DC converter-1, the first 4 inputs of six DABs are successively linked to the outputs of the phase A CHB converters and the other inputs of six DABs are successively linked to the primary two outputs of the segment B CHB converters; in addition, in DC/DC converter-2, the primary two inputs and the other four inputs of six DABs are successively connected to the latter two outputs of the phase B CHB converter and the outputs of the phase C CHB converter, respectively. The six DABs outputs in DC/DC converter-1 are associated together to load1; also, the six DABs yields in DC/DC converter-2 are associated together to load2.

The five-terminal hybrid AC/DC microgrid with four DC ports (DC port1, DC port2, DC port3 and DC port4) and one AC port is proposed in Fig. 1 and can be directly connected into three-phase medium-voltage grid. It consists of the AC/DC converter (CHB converters) and the compact DC/DC converter (DAB converters), composed of four group of DC/DC converters, namely DC/DC converter-1, DC/DC converter-2, DC/DC converter-3 and DC/DC converter-4. Considering the impact of various connection patterns of DAB converters, namely different wire connection between CHB converters outputs and DAB converters inputs, and different DAB submodules numbers in each DC/DC converter, the proposed five-terminal hybrid AC/DC microgrid has various types of internal structures. The DAB converter branches in various loads can be connected to the CHB cells' outputs randomly, where the issue of capacitor voltage unbalance will be solved by the proposed control scheme. Thus, the DAB converter connection patterns are not illustrated in Fig. 1.To further test the system performance of the proposed method, a modified five-terminal hybrid AC/DC micro grid with four DC ports is shown in Fig. 1.Considering various DC voltage demands, four voltage reference values are set as 750 V, 700 V, 600 V and 400 V respectively. Scenario 1 simulates the steady state with DC power matching (25 kW, denoted as P1) condition in the first 2 s; scenario 2 simulates the DC power mismatching (P1, 1.2*P1, 1.5*P1, 2*P1) condition from 2 s to 3 s; scenario 3 simulates the DC power mismatching and grid sags (grid voltage sags 50% in phase C) condition from 3 s to 4 s.

II. FIVE TERMINAL HYBRID AC/DC MICRO GRID

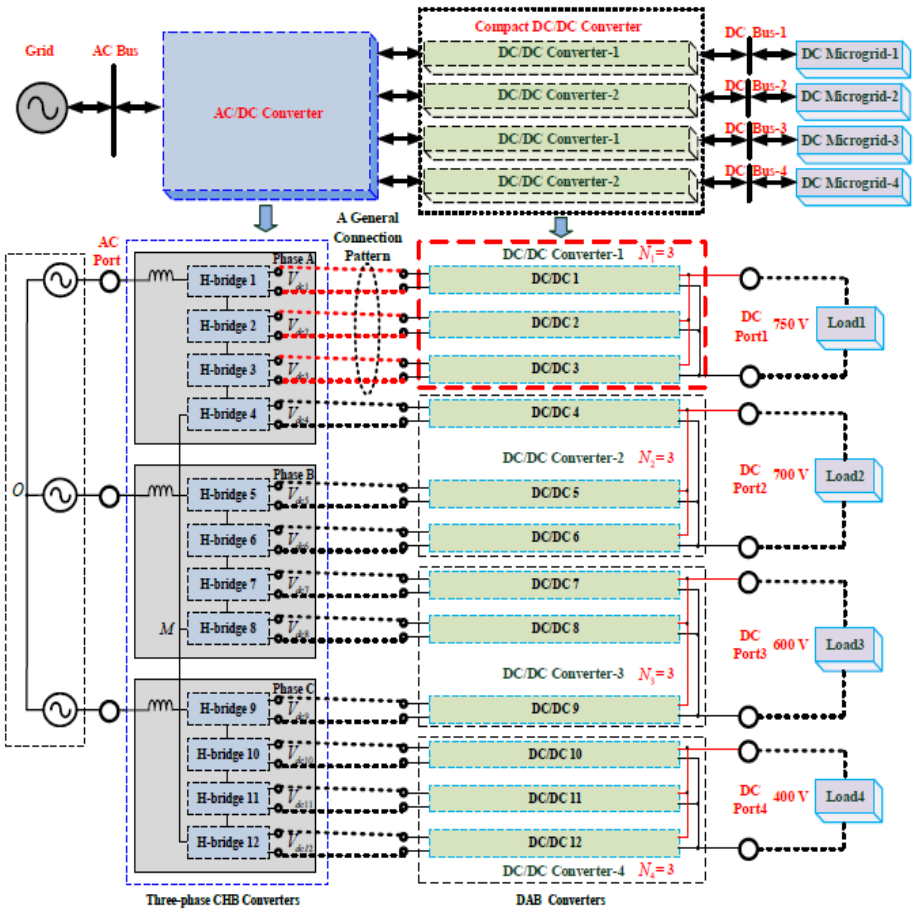

Fig.1. Five terminal Cascaded H-bridge Ac/Dc Micro Grid

The power unbalance problem of front-end CHB converters can be classified into two categories as follows: 1) the interphase (clustered) power unbalance, which occurs when each phase flows different power caused by mismatched DC network power or grid faults; 2) the inter-bridge (individual) power unbalance, which happens when each bridge in the same phase flows different power. With zero-sequence voltage injection (ZSVI), phasor diagram of front-end AC/DC converter with ZSVI in balanced operation is shown in Fig. 2. V_{gm} (m=a, b, c) is the grid voltage vector; V_{Lm} (m=a, b, c) is the inductor voltage vector; V_m (m=a, b, c) is the AC/DC converter voltage vector; I_{gm} (m=a, b, c) is the grid current vector; VOM is the zero-sequence voltage vector and γ is its phase angle; Fig. 2 reveals a critical fact that it is possible to rebalance these three-phase power by shifting the floating neutral point of three-phase converter from point M(O) to point M', which transfers the inter-phase power errors between overall average power of AC/DC converter and actual real power of each phase.

Define the injected zero-sequence voltage in the fundamental frequency as

$$V_{OM} = V_{OM} \cos(\omega t + \gamma) \quad (1)$$

III. ANALYSIS OF THREE TERMINAL HYBRID AC/DC MICRO GRID

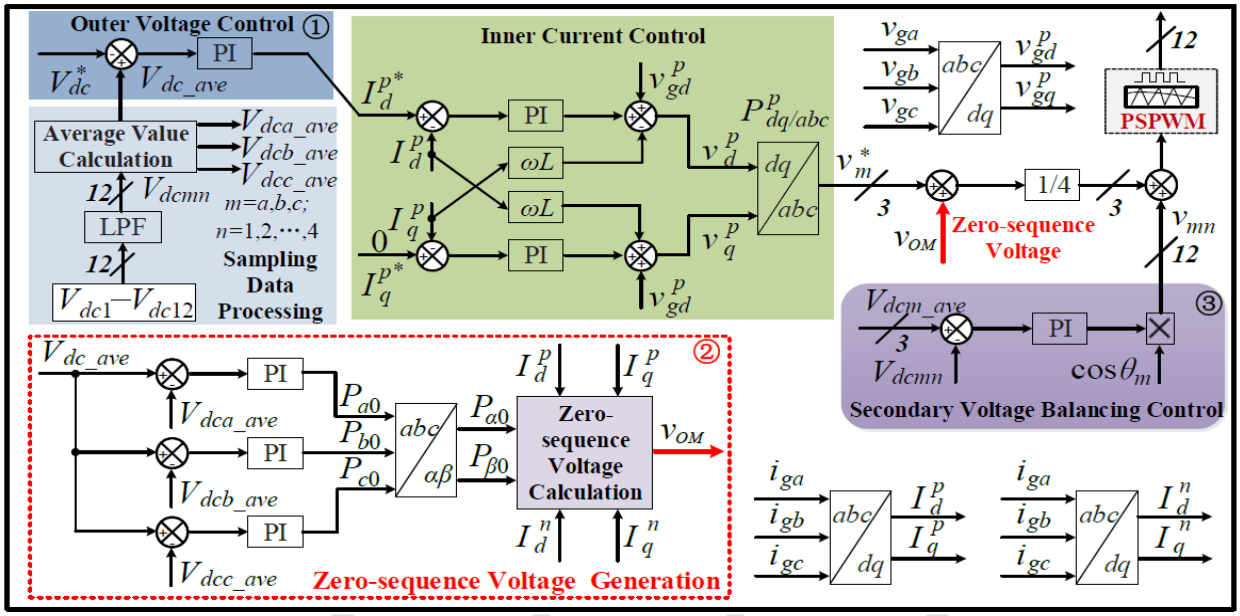

Fig.2. Analysis of Three terminal and five terminal controller

Where V_{OM} and γ are the magnitude and phase angle of zero-sequence voltage respectively; ω is angular frequency of grid. When the inductor voltage is neglected, three-phase converter phase-voltage in Fig. 1 can be expressed as

$$\begin{cases} V_{gaM} = v_{ga}^{p} + v_{ga}^{n} + v_{ga}^{o} = V_{gaO} + V_{OM} \\ V_{gbM} = v_{gb}^{p} + v_{gb}^{n} + v_{gb}^{o} = V_{gbO} + V_{OM} \\ V_{gcM} = v_{gc}^{p} + v_{gc}^{n} + v_{gc}^{o} = V_{gbO} + V_{OM} \end{cases} \quad (2)$$

Where $V_{gm\,M}$ (m=a, b, c) is the stage voltage of three-stage converter dependent on point M; V^{P}_{gm} , V^{n}_{gm} and V^{0}_{gm}(m=a, b, c) are the positive-, negative-and zero-arrangement part of each Stage voltage separately; V_{gmO}(m=a, b, c) is the aggregate of positive-and negative-grouping voltage of each stage voltage.

The PI controller based method in the five-terminal hybrid AC/DC micro grid is shown in Fig. 2. The feedback of all DC capacitor voltages V_{dcmn} (m=a, b, c; n=1, 2, 3, 4) are processed by the low-pass filter to reduce the double-line frequency ripples. Firstly, the average values of single-phase and three-phase DC voltages V_{dcm_ave} (m=a, b, c) and V_{dc_ave} are calculated by the block of average value calculation. Secondly, the controller of AC/DC converter is implemented by three control circles, i.e., external voltage control, zero-succession voltage age (ZSVG), and auxiliary voltage adjusting control. External voltage control plays out the general DC voltage control and manages the total power exchanged with grid; ZSVG realizes inter-phase power balance and adjusts the mismatched power among three phases, where the required dynamic zero-sequence voltage is calculated; secondary voltage balancing control achieves individual voltage balance and reallocates the different power among each bridge in the same phase. Thirdly, current controller is executed to obtain accurate current tracking and produce the required modulation voltage V^{*}_{m} (m=a, b, c). Then, these final PWM reference of each H-bridge cell v^{*}_{mn} (m=a, b, c; n=1, 2, 3, 4) are processed by the conventional phase-shift PWM (PSPWM) control to get the corresponding switching signals of AC/DC converter. Finally, the controller of DC/DC converters is performed by conventional phase-shift control method to get corresponding phase-shift angle. The phase-shift angle is regulated by a simple PI controller according to the voltage error between DC bus voltage and its voltage reference.

In the secondary voltage balancing control, by the PWM reference regulation value V_{mn} (m=a, b, c; n=1, 2, 3, 4), the product of corresponding phase angle θ_m (m=a, b, c) and PI controller output according to the voltage error between Vdcmn and Vdcm_ave, inter-bridge power is exchanged among H-bridge modules of the same phase to realize individual voltage balancing control.

The final modulation voltage in Fig. 1 can be described by

$$V^{*}_{mn} = \frac{1}{4}(V^{*}_{m} + V_{OM}) + V_{mn} \quad (3)$$

In the ZSVG, by PI controller according to the voltage error between Vdc_ave and Vdcm_ave, inter-phase power are exchanged among H-bridge modules of three phases. By these equations in (10)-(12), the required zero-sequence voltage is generated. By positive-sequence and negative-sequence Park transformation, three-phase grid currents i_{gm} (m=a, b, c) are transformed into the positive-sequence d-axis and q-axis currents I_{pd}, I_{pq} and negative-sequence d-axis and q-axis currents I_{nd}, I_{nq} respectively. The transient real power at each phase are defined as

$$P_{mn} = V_{gnO} i_{gm} \tag{4}$$

Where P_{mm} (m=a, b, c) are the transient power generated by V_{gmO} and I_{gm}. Thus, the corresponding average real power at each phase are calculated as

$$P_{mn} = \frac{\omega}{2\pi} \int_0^{2\pi/\omega} P_{mm}\, dt \tag{5}$$

Where P_{mm} (m=a, b, c) is the corresponding average power of P_{mm}. The overall average real power is calculated as

$$P_{ALL} = P_{aa} + P_{bb} + P_{cc} \tag{6}$$

$$= \frac{3}{2}\left(V_d^p I_d^p + V_q^p I_q^p + V_d^n I_d^n + V_q^n I_q^n\right) \tag{7}$$

Where P_{ALL} is overall average real power of three-phase converter; V_{pd} and V_{pq} are certain and negative-succession part of d-pivot voltage of lattice voltage; V n d and V n q are sure and negative-arrangement segment of q-axis voltage of grid voltage. The cluster average power is defined as

$$P_{Cm} = P_{mm} - \frac{P_{ALL}}{3} \tag{8}$$

Where P_{cm} (m=a, b, c) is the inter-phase power error between overall average active power of AC/DC converter and actual real power of each phase

$$P_{Ca} + P_{Cb} + P_{Cc} = 0 \tag{9}$$

Therefore, inter-phase power are wholly exchanged among three phases and no additional power is transmitted into three-phase converter. In the control process, the required zero-sequence voltage can be generated to readjust the inter-phase power in order to keep the inter-phase power balanced. Then, the cluster average power readjusted by ZSVI in the two-phase stationary frame is calculated as

$$\begin{bmatrix} P_{\alpha 0} \\ P_{\beta 0} \end{bmatrix} = P_{abc/\alpha\beta} \begin{bmatrix} P_{a0} \\ P_{b0} \\ P_{c0} \end{bmatrix}$$

$$= \frac{1}{2}\begin{bmatrix} I_d^p + I_d^n & -I_q^p + I_q^n \\ -I_q^p - I_q^n & -I_d^p + I_d^n \end{bmatrix} \begin{bmatrix} V_{OM}\cos\gamma \\ V_{OM}\sin\gamma \end{bmatrix} \tag{10}$$

Where Pm0 (m=a, b, c) is cluster average power readjusted by ZSVI in the three-phase stationary frame. Therefore, the d-axis and q-axis magnitude of V_{om} are calculated as

$$\begin{bmatrix} V_{OM}\cos\gamma \\ V_{OM}\sin\gamma \end{bmatrix} = k \begin{bmatrix} I_d^p + I_d^n & -I_q^p + I_q^n \\ -I_q^p - I_q^n & -I_d^p + I_d^n \end{bmatrix} \begin{bmatrix} P_{\alpha 0} \\ P_{\beta 0} \end{bmatrix} \tag{11}$$

$$k = \frac{2}{\left(I_d^n\right)^2 + \left(I_q^n\right)^2 - \left(I_d^p\right)^2 - \left(I_q^n\right)^2} \tag{12}$$

V_{OM} generated from above equation

$$V_{OM} = \sqrt{(V_{OM}\cos\gamma)^2 + (V_{OM}\sin\gamma)^2} \tag{13}$$

$$\gamma = \begin{cases} tan^{-1}\left(\dfrac{V_{OM}\sin\gamma}{V_{OM}\cos\gamma}\right) & V_{OM}\cos\gamma \geq 0; \\ tan^{-1}\left(\dfrac{V_{OM}\sin\gamma}{V_{OM}\cos\gamma}\right) + \pi & V_{OM}\cos\gamma < 0, V_{OM}\sin\gamma \geq 0; \\ \tan^{-1}\left(\dfrac{V_{OM}\sin\gamma}{V_{OM}\cos\gamma}\right) - \pi & V_{OM}\cos\gamma < 0, V_{OM}\sin\gamma < 0; \end{cases} \tag{14}$$

A. Outer Voltage Control:

Based on Fig. 2, the goal of outer voltage control is to generate the inner current references. When DAB converters are disconnected, total active power can be described

$$P_{ALL} \approx \frac{3}{2} v_D^P i_D^P = -3\,N\,I_C V_{DC} \quad (15)$$

Where I_c and V_{dc} are the current and steady-state voltage of DC capacitor in CHB converters respectively. Referring to (13) and Fig. 2, when the sample delay is neglected and three-phase system is balanced, control block diagram of outer voltage control based on Laplace transformation theory is shown. When accurate current tracking is achieved in the inner current control, its transfer function $G_{cpi}(s)$ can be approximately 1. Then, the closed transfer function can be expressed, the parameters of kp1 and ki1 can be determined and the corresponding design process is similar to that in the literature [25].

B. ZSVG:

Based on Fig. 2, three PI controllers are used to calculate the redistributed power for inter-phase power balance. To realize this control goal, the zero-sequence voltage is injected. This clustered balancing control based on ZSVG considers a cluster of single-phase cascaded converters in each phase as a single-phase H-bridge converter. Take phase A for example, the mathematical relationship between the clustered capacitor voltage and active power. When the sample delay is neglected, control block diagram of clustered balancing control based on ZSVG is shown. Then, this closed transfer function can be described as When components such as DAB converters and DC microgrids are connected to CHB converters outputs, the two control parameters of K_{p2} and K_{i2} are determined based on (16) and fine-tuning tests.

C. Secondary Voltage Balancing Control:

Based on Fig. 2, take phase A for example, define ΔV_{dcan} as the difference between the reference voltage (V_{dca_ave}) and the capacitor voltage of nth cell in the phase A CHB converters (ΔV_{dcan}). For simplification, K_{i3} is set as 0 at first in the design process of control parameters. In order to decrease ΔV_{dcan}, the compensating voltage can be given by

$$V_{an} = K_{p3} \Delta V_{dcan} \cos \omega t \quad (16)$$

Based on the assumption that I p d >> I_{pq}, I_{ga} can be approximately expressed as

$$i_{ga} = I_d^p \cos \omega t \quad (17)$$

Then, the active power of this cell to keep capacitor voltage balanced can be calculated as

$$P_{an} = v_{an} i_{ga} = D_{an} \quad (18)$$

Where Dan indicates the power loss or disturbance of this H-bridge cell [25]. Whose goal is to realize individual voltage balancing control, this closed transfer function can be described as

$$\frac{\Delta V_{dcan}(s)}{D_{an}(s)} = \frac{1}{CV_{dc} + K_{p3} I_d^p / 2} \quad (19)$$

Based on (11), the control parameters of Kp3 and Ki3 are determined and the similar design process can be found in reference [16].

IV. SIMULATION RESULTS AND DISCUSSIONS

An Adaptive neuro-fuzzy inference system is a kind of artificial neural network that is based on Sugeno fuzzy inference system for using the ANFIS is more efficient and optimal way, one can use the best parameter obtained by genetic algorithm and it is a simple data learning technique that uses a fuzzy inference system model to transform a give input into a target output. Scenario 1 simulates the steady state with matched loads in the first 2 s; scenario 2 simulates the case of load mismatching from 2 s to 3 s; scenario 3 simulates the case of load mismatching and grid sags (grid voltage sags 50% in phase C) from 3 s to 4 s. The prediction involves membership function, fuzzy logic operators and if-then rules. This learning technique works also to that of neural systems. ANFIS is fuzzy Sugeno demonstrate put in the structure to encourage learning and adjustment methodology. Such system makes fuzzy rational more orderly and less depending on master information. The goal of ANFIS is to change the parameters of a fuzzy grid by applying a learning method utilizing input– yield preparing information. Essential design of ANFIS that has two information sources x and y and one yield f. In MATLAB the primary distinction between fuzzy controller and versatile neuro fuzzy controller is just we have in Mat lab two writes fuzzy controllers one is Mamdani and second one is Sugeno. Mamdani is common fuzzy controller in this we give info and yield by utilizing a few suppositions yet in Sugeno compose we give inputs just they naturally

prepare yields this is the primary contrast between two fuzzy controllers in Mat lab. So Mamdani compose fuzzy controller utilized as customary fuzzy controller and Sugeno write fuzzy controller utilized as versatile neuro fuzzy controller in MATLAB.

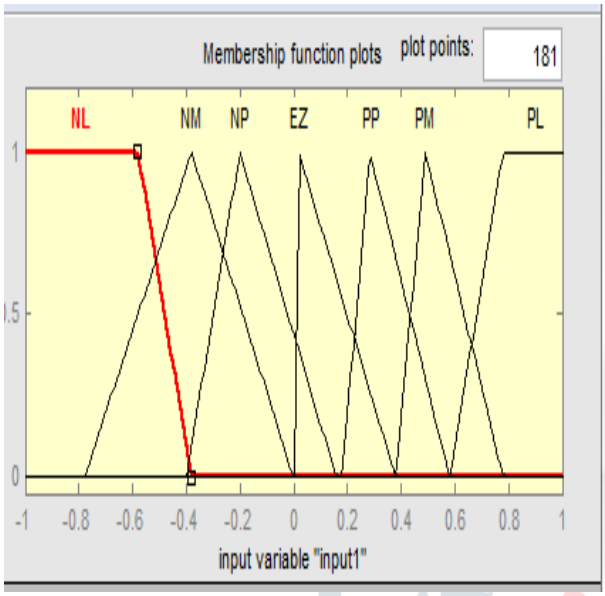

Fig.3. Input membership function-1

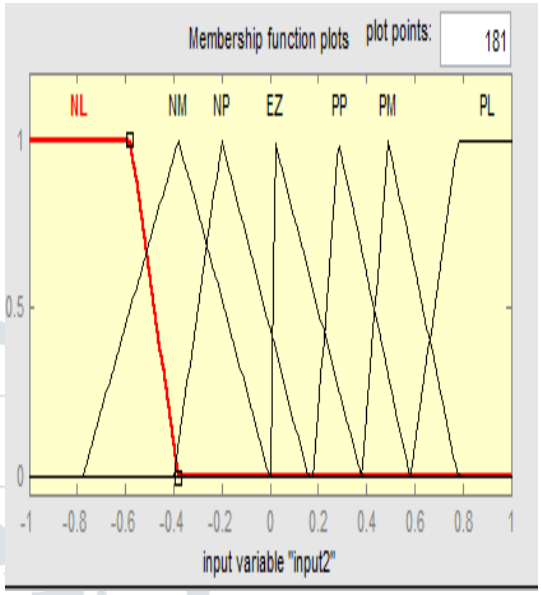

Fig.4. input membership function-2

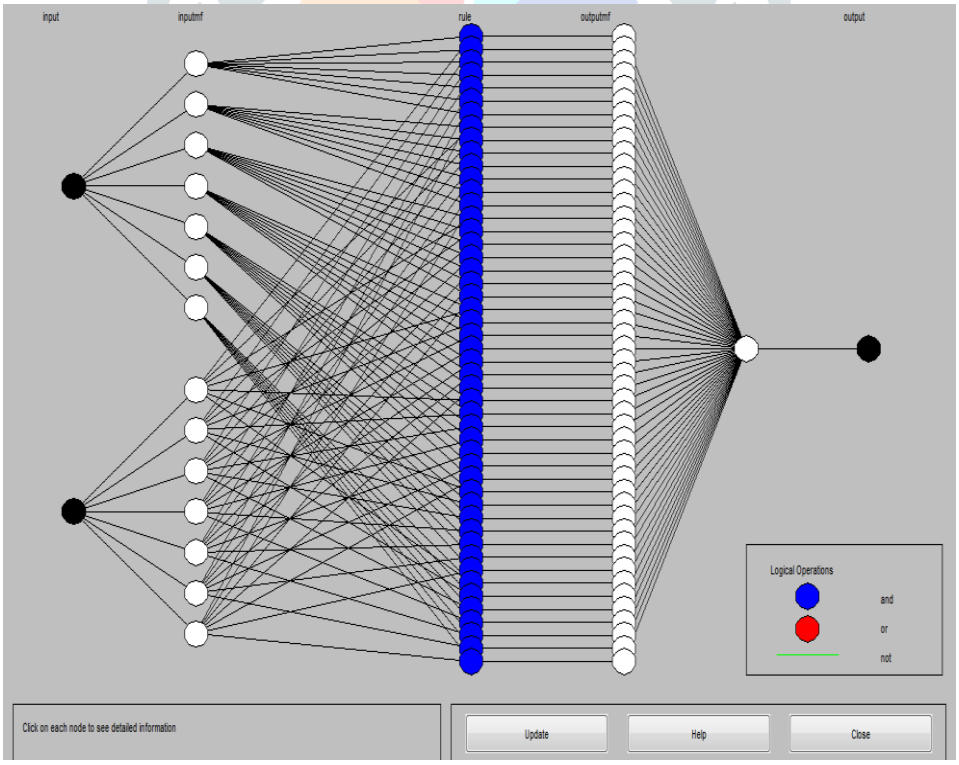

Fig.5. ANFIS structure

Table 1. Fuzzy Truth table

dE / E	NL	NM	NS	EZ	PS	PM	PL
NL	NL	NL	NL	NL	NM	NS	NL
NM	NL	NL	NL	NM	NS	EZ	NM
NS	NL	NL	NM	NS	EZ	PS	NS
EZ	NL	NL	NS	EZ	PS	PM	EZ
PS	NM	NM	EZ	PS	PM	PL	PS
PM	NS	NS	PS	PM	PL	PL	PM
PL	EZ	EZ	PM	PL	PL	PL	PL

A. Five Terminal Controller System

Investigation of three terminal cross breed AC/DC smaller scale lattice by utilizing anfis controller demonstrated as follows. The results of ANFIS controller like improved network current and voltage adjusting execution demonstrated as follows.

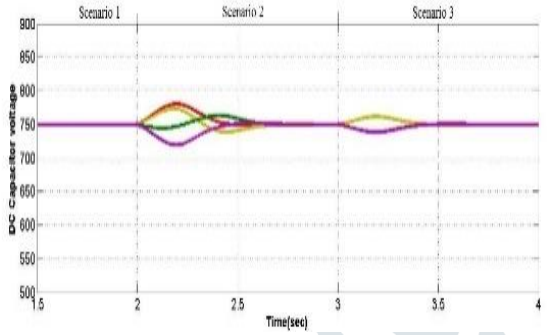

Fig.6a. Dc capacitor voltage of AC/DC by the existing method

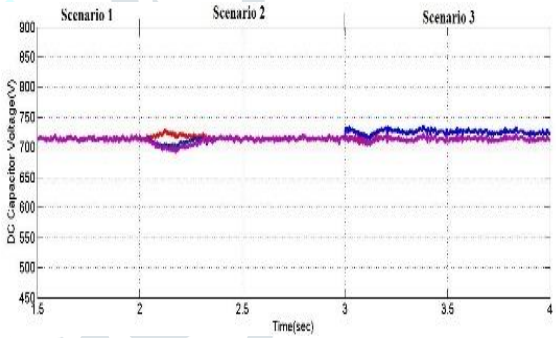

Fig.6b. Dc capacitor voltage of AC/DC by the proposed method

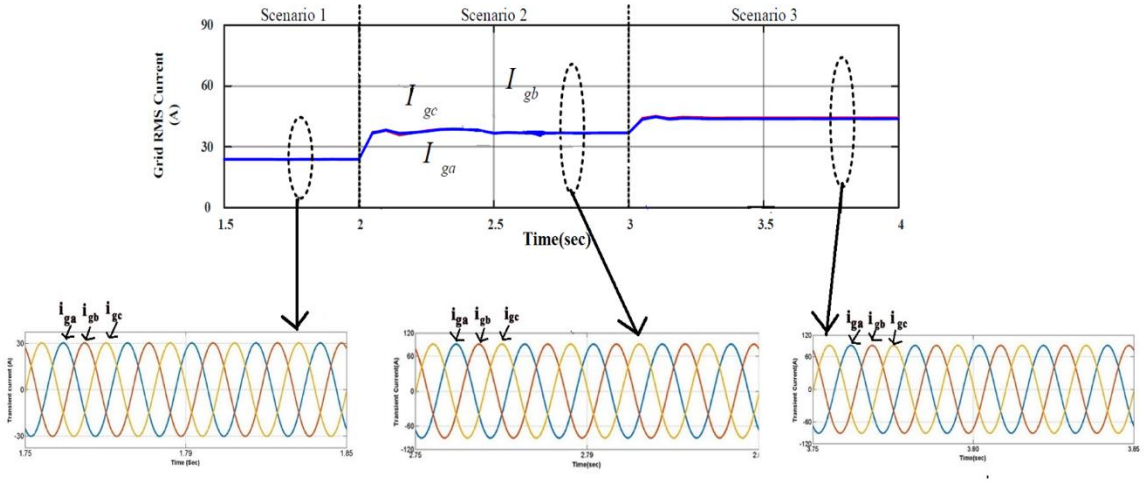

Fig.7.phase grid RMS currents and transient values by the existing method

In figure 6 b. we can clearly see that there is less sag less swell in the DC capacitor voltage as compared to the existing method in scenario 2. However by the proposed method the outer voltage control is injected to change these ANFIS values of AC/DC converter and final switching values of power modules are adjusted.

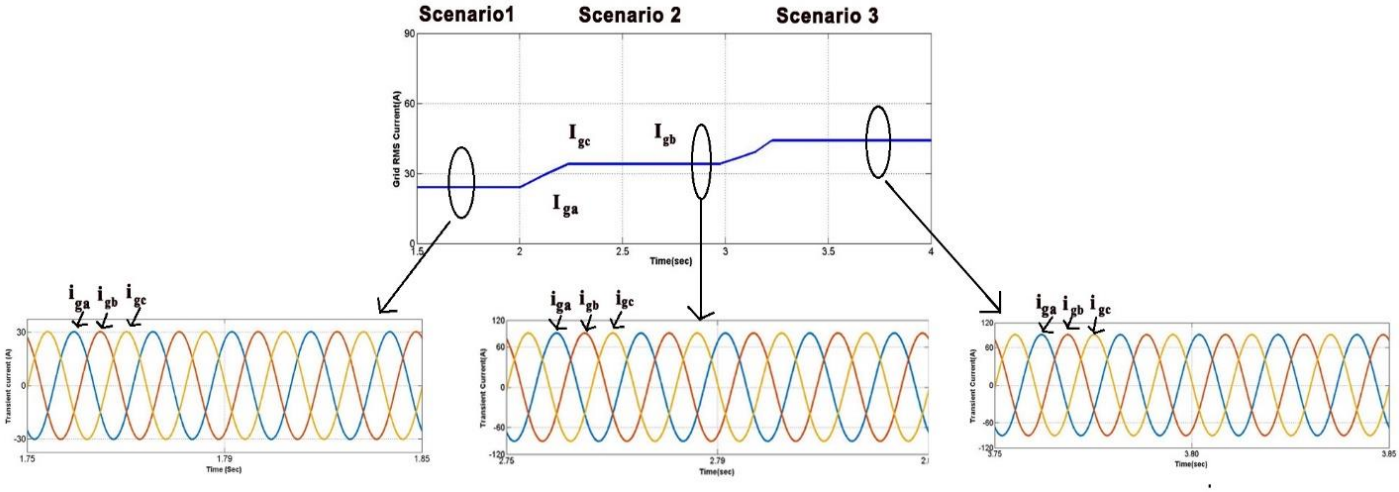

Fig.8. Three-phase grid RMS currents and transient values by the proposed method

Three phase grid RMS currents and transient values by the existing method are shown in Fig.7. It is easily observed that compare to Fig.17. We observed in Fig.8. a smooth transient of grid RMS current magnitude change from scenario 1 to scenario 2 and scenario 2 to scenario.

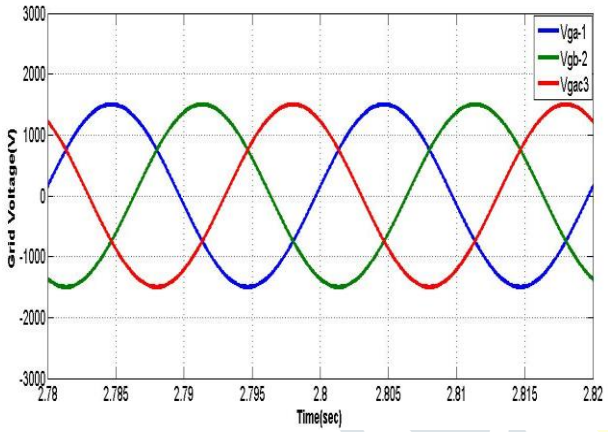

Fig.9a Grid Voltage-1

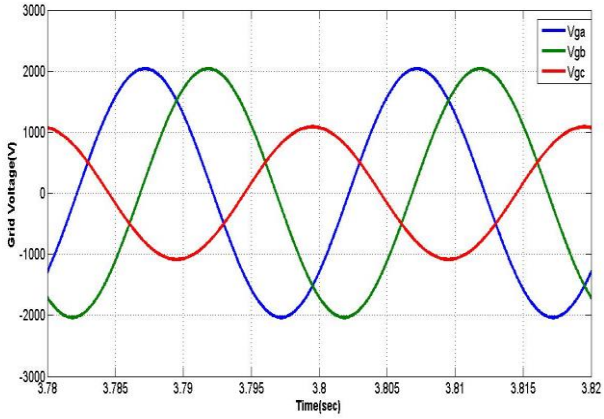

Fig.9b Grid Voltage-2

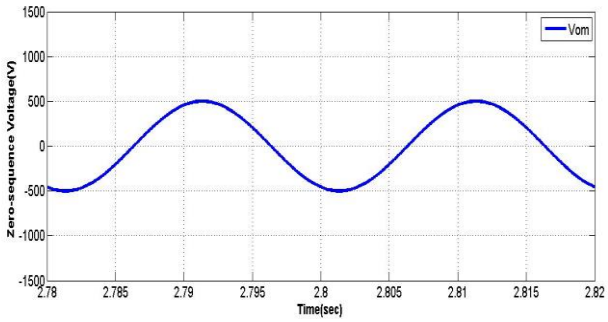

Fig.9.c Vom-1

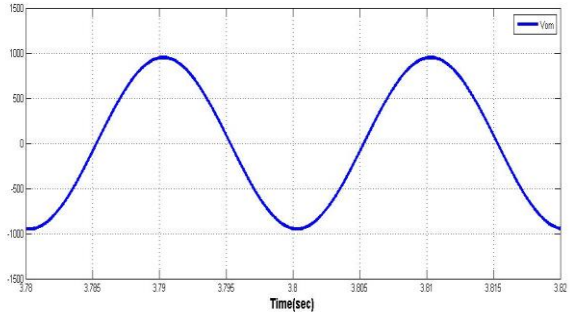

Fig. 9d. Vom-2

Fig.9. Dynamic zero-sequence voltage and three-phase grid voltages by the existing method.

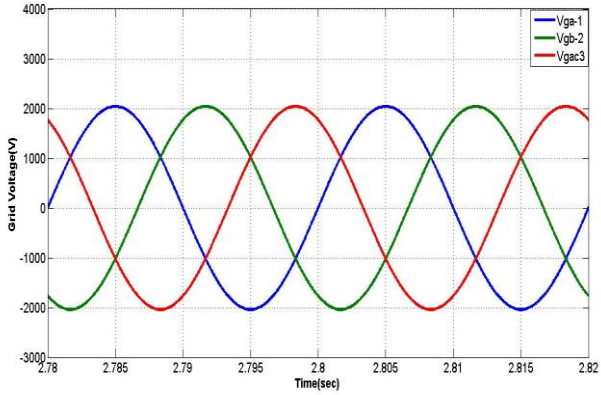

Fig.10a Grid Voltage-1

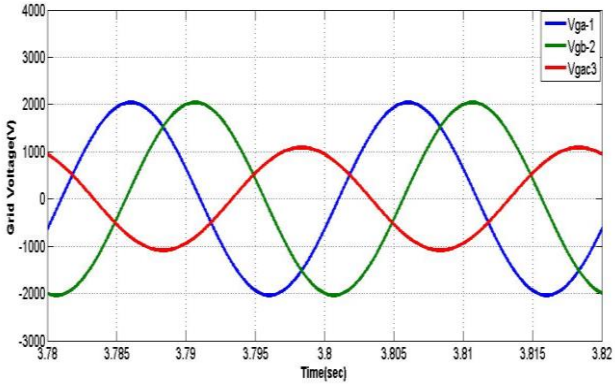

Fig.10b Grid Voltage-2

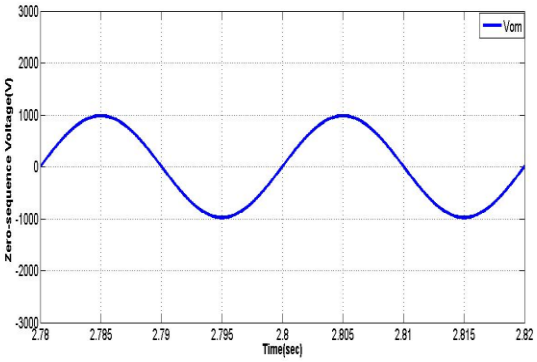

Fig.10c Vom-1

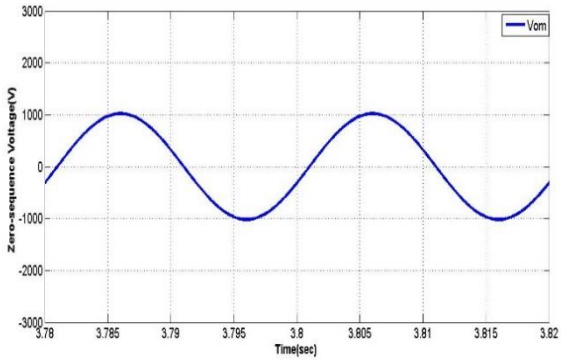

Fig.10d Vom-2

Fig.10. Dynamic zero-sequence voltage and three-phase grid voltages by the proposed method

To overcome the unbalance problem of AC/DC caused by mismatch DC voltage and grid sags is overcome by injecting dynamic zero-sequence voltage into front end of converter the grid voltage is improved 1200v to 1800v as shown in Fig. 10.a, the dynamic zero-sequence voltage is injected into modulation signals of front end CHB.

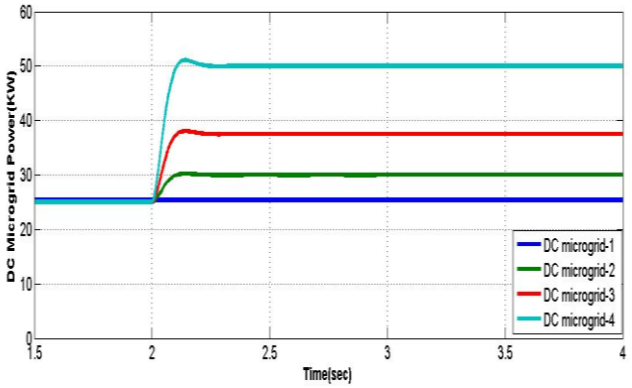

Fig.11a. DC micro grids power by the existing method

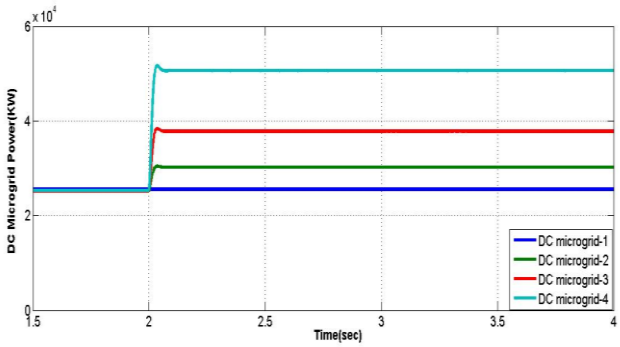

Fig.11b. DC micro grids power by proposed method

By the proposed method, four DC micro grids power and DC bus voltages of DAB converter are shown in Fig.11b. we can clearly observe that after that DC bus voltage mismatch it took 0.25sec to attain the respective bus voltages in Fig.11b. after the DC bus voltage mismatch we observe that 0.08sec bus attain the respective voltage.

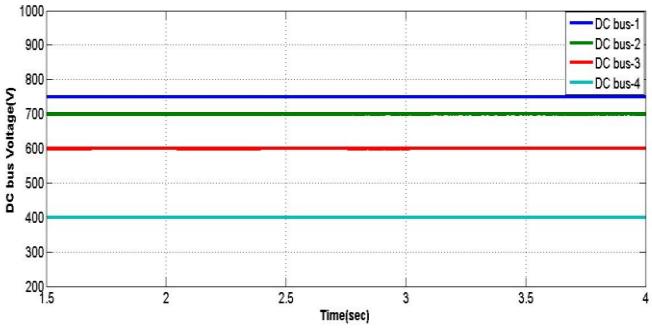

Fig.12a. DC bus voltages of DAB converter by existing system

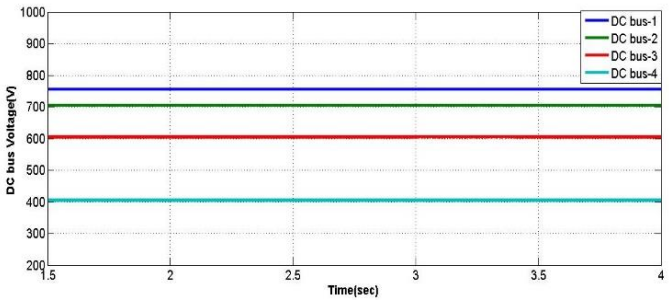

Fig.12b. DC bus voltages of DAB converter by proposed system

It is noted that mismatched power of DC microgrid-1, DC microgrid-2, DC microgrid-3 and DC microgrid-4 is simulated based on the identical DC bus voltage(700V).Then, different DC bus voltages can also be set according to the desired DC voltages, shown in Fig.12b.

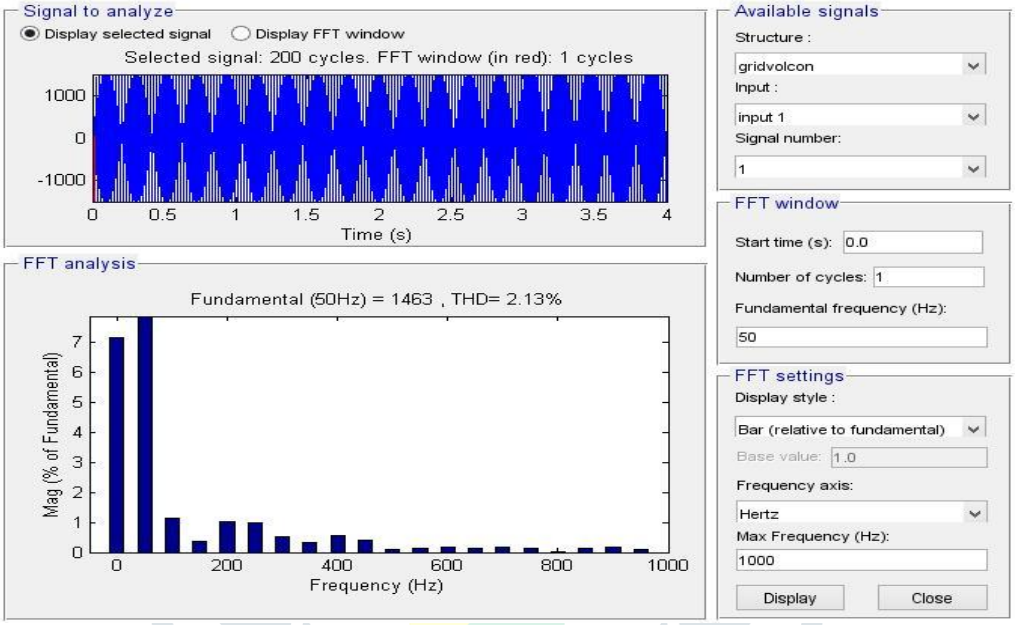

Fig. 13. Evaluation of THD for existing system

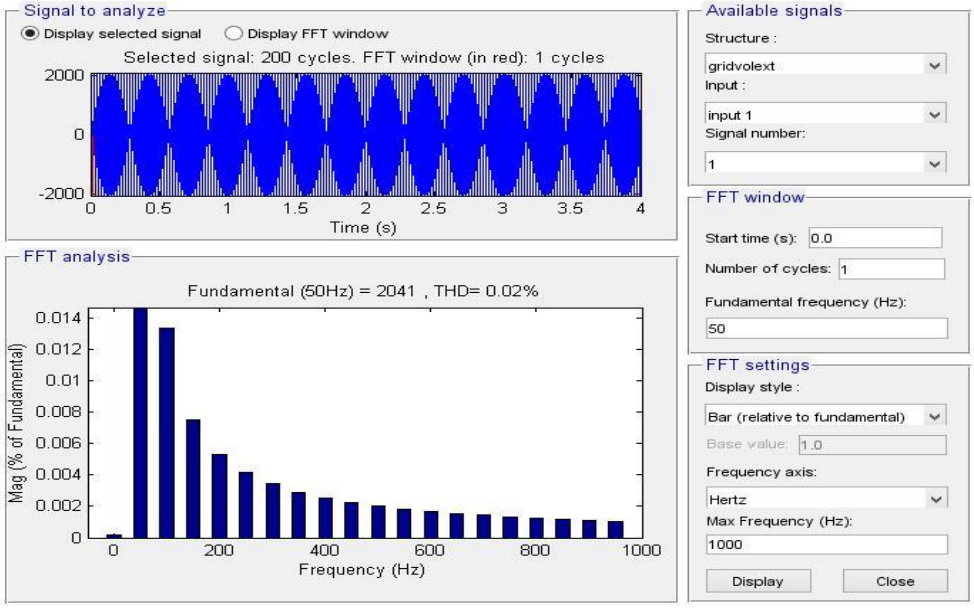

Fig.14.Evaluation of THD for proposed system

V. CONCLUSION

In this paper to improve the grid current and DC capacitor voltage balancing by using ANFIS controller. The main achievement decrease the number of stages and losses also. In this project mainly study about three terminal based and five terminal based CHB terminals. The main problems facing unbalance voltage and grid currents by using this controller getting better results. It has been extensively verified that the grid current and CHB capacitor voltage balancing control can be achieved simultaneously

even in the severe case with highly mismatched DC power, grid-voltage sags, or the changes of connection between AC and DC sub grids.

Table 2. Comparison of performance parameters

	PI Controller	**ANFIS**
%THD	2.13%	0.02%
Execution Time	2.2 Sec	2.0 Sec

Future Scope:

Despite reduced harmonics by the use of ANFIS controller, the harmonics are still present to some extent. These harmonics can be still further eliminated by the use of Artificial Neural Network.

VI. REFERENCES

[1]P. Ch. Loh, D. Li, Y. K. Chai, and F. Blaabjerg, "Autonomous operation of hybrid microgrid with AC and DC subgrids," IEEE Trans. Power Electron., vol. 28, no. 5, pp. 2214–2223, May. 2013.
[2]P. Ch. Loh, D. Li, Y. K. Chai, and F. Blaabjerg, "Autonomous control of interlinking converter with energy storage in hybrid AC–DC microgrid," IEEE Trans. Ind. Appl., vol. 49, no. 3, pp. 1374–1383, May. 2013.
[3]Y. W. Li, D. M. Vilathgamuwa, and P. C. Loh, "Design, analysis and real-time testing of controllers for multi-bus microgrid system," IEEE Trans. Power Electron., vol. 19, no. 5, pp. 1195–1204, Sep. 2004.
[4]J. M. Guerrero, J. C. Vasquez, J. Matas, L. G. de Vicuna, and M. Castilla, "Hierarchical control of droop-controlled AC and DC microgrids—Ageneral approach toward standardization," IEEE Trans. Ind. Electron.,vol. 58, no. 1, pp. 158–172, Jan. 2011.
[5]K. T. Tan, X. Y. Peng, P. L. So, Y. C. Chu, and M. Z. Q. Chen, "Centralized control for parallel operation of distributed generation inverters in microgrids," IEEE Trans. Smart Grid, vol. 3, no. 4, pp. 1977–1987, Dec.2012.
[6]B. Wang, M. Sechilariu, and F. Locment, "Intelligent DC microgrid with smart grid communications: Control strategy consideration and design," IEEE Trans. Smart Grid, vol. 3,
[7]X. Liu, P. Wang, and P. C. Loh, "A Hybrid AC/DC micro grid and its coordination control," IEEE Trans. Smart Grid, vol. 2, no. 2, pp. 278–286, Jul. 2011.
[8]J. He, Y. Li, J. Guerrero, F. Blaabjerg, and J. Vasquez, "An islanding microgrid power sharing approach using enhanced virtual impedance control scheme," IEEE Trans. Power Electron., vol. 28, no. 11, pp. 5272–5282, Nov. 2013.
[9]X. Lu, J. M. Guerrero, and K. Sun, "An improved droop control method for DC microgrids based on low bandwidth communication with DC bus voltage restoration and enhanced current sharing accuracy," IEEE Trans. Power Electron., vol. 29, no. 4, pp. 1800–1813, Apr. 2014.
[10]J. Rocabert, A. Luna, F. Blaabjerg, and P. Rodriguez, "Control of power converters in ac microgrids," IEEE Trans. Power Electron., vol. 27, no. 11, pp. 4734–4749, Nov. 2012.
[11]C. S. Wang, X. L. Li, L. Guo, and Y. W. Li, "A nonlinear-disturbance-observer-based DC-bus voltage control for a hybrid AC/DC microgrid," IEEE Trans. Power Electron., vol. 29, no. 11, pp. 6162–6177, Nov. 2014.
[12]K. Kurohane, T. Senjyu, A. Yona, N. Urasaki, T. Goya, and T. Funabashi, "A hybrid smart AC/DC power system," IEEE Trans. Smart Grid, vol. 1, no. 2, pp. 199–204, Sep. 2010.
[13]F. Nejabatkhah, Y. W. Li, "Overview of power management strategies of hybrid AC/DC microgrid," IEEE Trans. Power Electron., vol. 30, no. 12, pp. 7072–7089, Dec. 2015.
[14]M. Li, M. M. Tong, J. E. Fletcher, and Z. Y. Dong, "A novel approach to investigate the deterioration of insulation of oils in power transformers with terahertz time-domain spectroscopy," IEEE Trans. Dielectr. Electr. Insul., vol. 24, no. 2, pp. 930–938, Apr. 2017.
[15]J. J. Dai, H. Song, G. H. Sheng, and X. C. Jiang, "Dissolved gas analysis of insulating oil for power transformer fault diagnosis with deep belief network," IEEE Trans. Dielectr. Electr. Insul., vol. 24, no. 5, pp. 2828–2835, Oct. 2017
[16]Y. Liu, A. Q. Huang, W. C. Song, S. Bhattacharya, and G. J. Tan, "Small-signal model-based control strategy for balancing individual DC capacitor voltages in cascade multilevel inverter-based STATCOM," IEEE Trans. Ind. Electron.,vol. 56, no. 6, pp. 2259–2269, Jun. 2009.

AUTHOR'S PROFILE

Ms Ananya Bakkachinnayagari has graduated her B.Tech from Vaagdevi Institute of Technology and Science, Proddatur, YSR Kadapa, A.P. Currently her is pursuing M.Tech (Electrical Power Systems) from Sri Krishnadevaraya University college of Engineering and Technology, S.K.University, Ananthapuramu-515 003, A.P, India. Her areas of interest are Power Systems and Renewable Energy Sources.

Mr. P. SHASHAVALI Received his B.Tech Degree from the JNT University Hyderabad. He received Master of Technology degree from G. Pulla Reddy Engineering College Kurnool. Currently he is Pursuing Ph.D degree from JNT University Anantapur. Presently, he is working as Assistant Professor in the Department of Electrical and Electronics Engineering, S.K.University College of Engineering & Technology, S.K.University, Ananthapuramu-515 003, Andhra Pradesh, India. His research area of interest is Reliability concepts in Power Electronic Converters, Renewable Energy Sources and Facts Devices.

Mr. N. RAJESH KUMAR GOWD has graduated his B.Tech from St. John's College of Engg & Tech, Kurnool, A.P, India and M..Tech (EPE) from Bharath institute of Engineering and Technology Ibrahimpatnam, Hyderabad, T.S, India. Presently he is working as Lecturer in Dept of EEE in Sri Krishna Devaraya University college of Engineering and Technology, Ananthapuramu – 515 003, A.P., India. He has published 7 International Journals & 3 National conferences. His research areas of interest are Electrical Power System-Smart grid, Reliability, Power electronics design.